Article

Theoretical Assessment of the Risk of Ocular Hypotony in Patients With Intravitreal Gas Bubbles Who Travel Through Subsea Tunnels

Neda Rashidi[1],*, Vineet S. Thomas[1],*, and Rouzbeh Amini[1]

[1] Department of Biomedical Engineering, The University of Akron, Akron, OH, USA

Purpose: This study was conducted to investigate changes in intraocular pressure (IOP) in the presence of intravitreal gas bubbles in individuals who travel through subsea tunnels.

Methods: Using a mathematical model, we simulated alterations in ocular globe shape, aqueous humor flow, volume of intravitreal gas bubbles, and IOP due to elevation changes during travel through subsea tunnels. We simulated five tunnels with different features as case studies. The role of key modeling parameters was further evaluated in a parametric study.

Results: In three out of the five simulated tunnels (i.e., Seikan Tunnel, Bomlafjord Tunnel, and the Atlantic Ocean Tunnel), the patients were potentially at risk at lower portions of the tunnels since the IOP dropped to values less than 5 mm Hg, the clinical threshold for ocular hypotony. During ascent, the IOP increased to the normal value of 15 mm Hg and in some cases to higher values (e.g., a peak value of 22 mm Hg in Seikan Tunnel).

Conclusions: Our model predicted that in the presence of intravitreal gas bubbles, the IOP could drop to extremely low values when patients descend to lower elevations in some tunnels. Such low IOP values could cause bleeding and/or retinal detachment. Since many factors (e.g., tunnel specifications and/or patient-specific characteristics) could affect the IOP during subsea travel, caution (beyond avoiding airplane flights) should be taken in advising patients about travel restrictions following intravitreal gas injections.

Translational Relevance: Our findings highlight the potential risk for hypotony in the presence of intravitreal gas bubbles during subsea travels.

Introduction

Vitreous traction on the retina creates retina breaks, which can lead to the accumulation of fluid in the subretinal space. Retinal breaks and the subsequent accumulation of fluids may cause the neurosensory retina layer to become separated from its underlying retinal pigment epithelium layer, a condition known as rhegmatogenous retinal detachment (RRD), and could lead to permanent vision loss.[1] Epidemiological analyses have shown that RRD incidence varies in different regions, and its annual incidence has been reported to be within the range of 6.3 to 17.9 per 100,000 people among different

ethnicities and ages.[2] The retina can be reattached via a variety of procedures, many of which involve the injection of a gas bubble in the vitreous humor. Buoyancy and surface tension forces due to the presence of the gas bubble will aid in the reattachment of the retina.[3,4] Reabsorption of gas bubbles will typically occur within 12 to 38 days after the procedure without the need for additional surgeries.[3]

Although intravitreal gas injection is an efficient method for treating retinal detachment, complications may arise if patients engage in activities that involve changes in elevation within a few days after the procedure. In particular, according to the Boyle's law, when gases are subjected to elevation-induced pres-

sure variations, the pressure and volume are inversely related at a constant temperature. Due to the encapsulation of the gas bubble within the ocular globe, other parameters such as ocular globe deformation and changes in ocular fluid volume (i.e., aqueous humor, vitreous humor, and blood) affect the bubble volume and the intraocular pressure (IOP).[5] Maintaining a normal IOP value (between 10 and 20 mm Hg) is necessary for a number of physiological functions of the eye and is achieved by the circulation of the aqueous humor within the anterior segment and through the trabecular meshwork.[6] However, an increase in elevation may lead to higher values of IOP due to the drop in atmospheric pressure and the expansion of the gas bubble,[7–9] causing headaches and discomfort and potentially putting the patient at risk.[10] As such, following intravitreal gas injections, patients are strongly advised to avoid travel to places at high altitudes and to avoid flying in airplanes.

Recently, case reports and our theoretical models have shown that even if the patient travels to a low altitude and subsequently returns to the initial elevation (without ever exceeding the initial elevation), the peak IOP values may surpass the normal values.[11,12] As such, we have demonstrated that the change in altitude (and not necessarily the absolute height of the elevation) can lead to high values for the IOP. In the current study, we have further investigated trips that involve traveling to lower altitudes, with a focus on the potential for development of ocular hypotony. Clinically, ocular hypotony has been defined by some as a condition in which the IOP drops below 5 mm Hg.[13] Ocular hypotony can lead to a number of ocular complications and is especially dangerous for patients who have recently undergone retinal detachment procedures. In particular, ocular hypotony may cause buckling of the scleral shell and put the patients at high risk for re-detachment of the retina.

In this investigation, we chose five subsea tunnels as case studies of typical transportation methods that may put patients with intravitreal gas bubbles at risk for ocular hypotony. While previous studies were conducted to investigate the potential for dangerous peak values of IOP induced by changes in elevation,[5,7,9,11,12,14,15] to our knowledge, the occurrence of ocular hypotony in the presence of intravitreal gas bubbles has not yet been studied. In our assessment of the changes in IOP during travel through these five subsea tunnels, we also investigated how the occurrence of ocular hypotony can be influenced if model parameters such as aqueous humor filtration or production rates are decreased/increased from their base mean values.

Methods

We previously developed a computational framework to predict changes in IOP during both ascent and descent in the presence of intravitreal gas bubbles.[9,11] The model was divided into two regions based on their compressibility: an incompressible region representing the lens, aqueous humor, and vitreous humor and a compressible region representing the gas bubble. The initial volume of the globe was considered as 7211 µL.[11] Since aqueous humor outflow and inflow are both pressure dependent and can affect ocular volume, the change in the aqueous flow was also incorporated in the model. The trabecular meshwork, the primary site of outflow, was treated as a pressure dependent one-way valve.[11] Additional details about this model are provided in the Appendix.

We have previously examined the fidelity of our model using data from a single patient with an initial bubble size of 65% of the globe volume.[9] This model predicted IOP values during an ascent from sea level to 3000 ft and a descent back to sea level that were consistent with published experimental data.[16] Moreover, in our recent study,[9] we used the same model for simulating IOP in four patients who travel to lower altitudes based on the parameters from a published case report.[12] The detailed IOP data for the entire trip were not provided in the case report. However, the peak IOP value resulting from a descent to low elevations and a return ascent without exceeding the surgical elevation was reported, and it compared well with our simulated values.[12] In this study, we implemented our model to predict IOP changes as a patient travels through five different subsea tunnels.

The five tunnels were chosen to represent different geographical locations (i.e., Asia, Europe, and America) and different tunnel profiles (e.g., rapid descent versus slow descent and short trips [~3 minutes] versus long trips [~25 minutes]). The five tunnels used in the simulation are:

1. Seikan Tunnel, a 53,850-m tunnel that connects Aomori Prefecture on the main island of Japan (Honshu) to the northern island of Hokkaido.[17]
2. Bomlafjord Tunnel, a 7900-m tunnel that connects the island of Foyno in Stord to the mainland at Dalshovda in Sveio, Norway.[18,19]

Table 1. Parameters Used to Simulate the Travel in Five Different Tunnels

Tunnel	Elevation			Rate of Descent (m/min)	Rate of Ascent (m/min)	Initial Gas Bubble Size (%)	Design Speed (m/min)
	Entrance (m)	Lowest Point (m)	Exit (m)				
Seikan Tunnel	32	−240	82	25	26	70	2330
Bomlafjord Tunnel	42	−260	8	113	84	70	1330
Channel Tunnel	55	−115	10	18	13	70	2670
Ted Williams Tunnel	6	−30	4	39	28	70	1200
Atlantic Ocean Tunnel	27	−250	−50	115	105	70	1330

3. Channel Tunnel (also known as "the Chunnel"), a 49,300-m tunnel that connects Folkestone (UK) to Coquelles (Northern France).[20]
4. Ted Williams Tunnel, a 2600-m tunnel that connects South Boston to Logan International Airport (part of the "Big Dig" project) in Boston, USA.[21,22]
5. Atlantic Ocean Tunnel, a 5700-m tunnel that connects the towns of Kristiansund and Averoy in More og Romsdal County, Norway.

Tunnel specifications, including the elevation at the beginning and end of each tunnel as well as the altitude at the lowest part of each tunnel, are listed in Table 1.

The variables used in the theoretical model are described in Table 2. Details of our theoretical model, including the governing equations, are presented in the Appendix. Briefly, a time–altitude vector corresponding to each tunnel was used as the input for our model. The values for elevation at the tunnel entrance, the elevation at the lowest point, and the elevation at the tunnel exit were entered into the model based on the tunnel altitude profiles shown in

Table 2. Variables Used in the Theoretical Model

Symbol	Description
α_0	Ratio of initial bubble volume to initial globe volume
h	Elevation
P_{out}	Absolute exterior air pressure
P_{in}	Absolute intraocular (interior) pressure
$P0_{out}$	Initial absolute exterior air pressure
$P0_{in}$	Initial absolute intraocular (interior) pressure
P_e	Absolute episcleral venous pressure
V_B	Bubble volume
V_{globe}	Ocular globe volume
V_{Aqu}	Aqueous humor volume

Figures 1a–1e. Ascent rates and descent rates were calculated based on the maximum design speeds and the tunnel elevation profiles. The initial gas bubble size was chosen as 70% for all tunnel simulations listed in Table 1. A normal IOP of 15 mm Hg was considered as the baseline value at the entrance to all simulated tunnels.

As discussed in our previous publication,[9] since the mechanism of both inflow and outflow of the aqueous humor are pressure-dependent,[23–25] we have included the aqueous flow changes due to the IOP control mechanisms in our model. For example, the conventional trabecular meshwork outflow was treated as a pressure-dependent one-way valve.[9] Further, consistent with clinical conventions, an IOP of less than 5 mm Hg was considered as ocular hypotony.[13] Extreme cases of ocular hypotony (i.e., negative IOP), however, were prevented in our model as described in detail in our previous paper.[11] Such a constraint was applied because negative IOP is not physiologically possible.[26]

Previous studies have shown that the compliance of the ocular globe can vary, ranging from approximately 1 to 4 μL/mm Hg.[27] For our model, deformation of the ocular globe was assumed to be linear elastic with a compliance of 3.115 μL/mm Hg, as discussed previously.[11] A constant outflow facility of 0.25 μL/min mm Hg was used. Table 3 presents a complete list of input parameters and their corresponding values. The governing equations were described in detail in our previous work.[9,11]

A parametric study was performed for the key parameters of the base model for each tunnel (as listed in Table 3). Similar to a previous study,[28] the purpose of the parametric study was to investigate how perturbation of the model parameters from the baseline values would affect the simulation predictions. The key parameters were chosen in part because of their potential for variation due to physiological
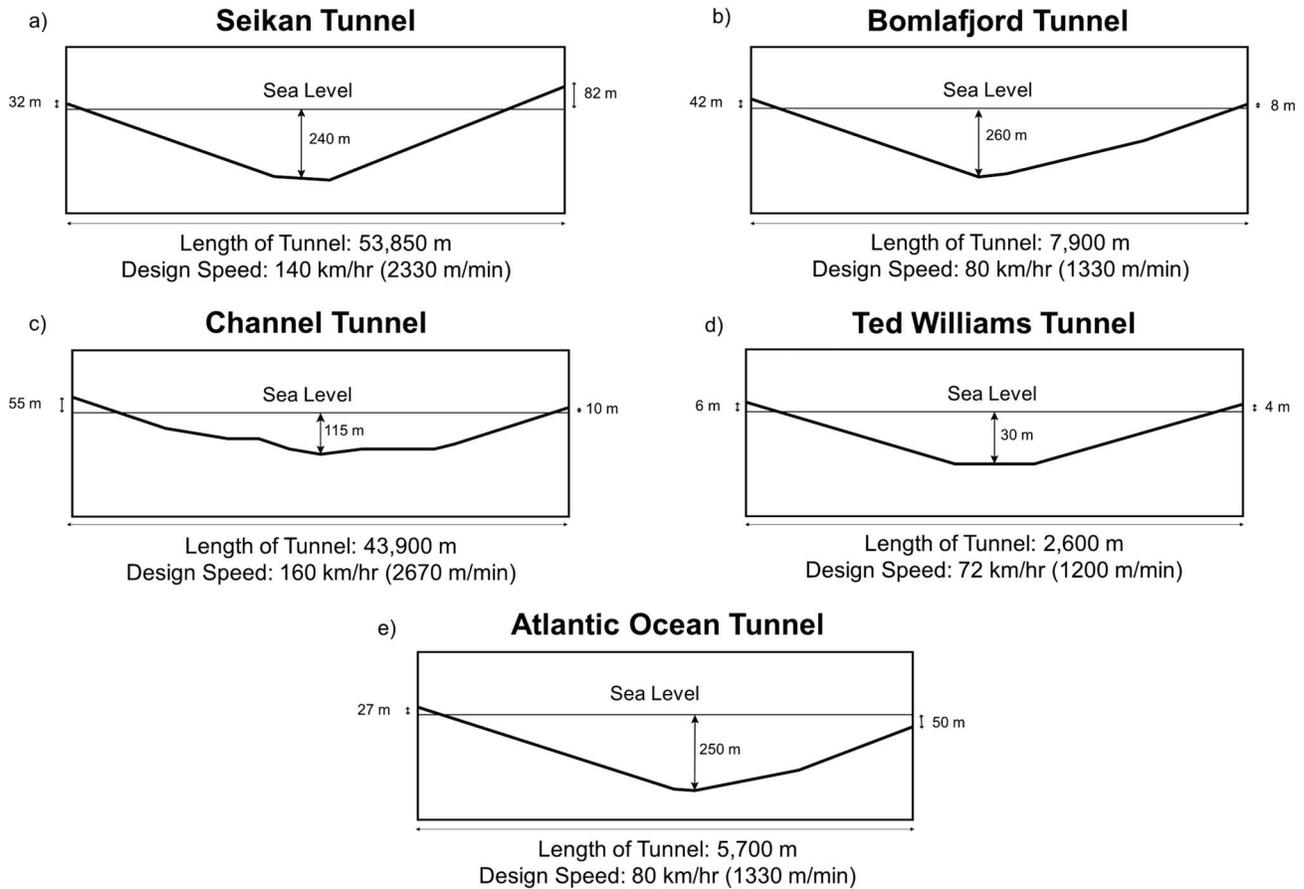
Figure 1. Schematics of the tunnel profiles used as case studies.

(or drug-induced) effects or based on different travel scenarios (e.g., exceeding the posted speed limit or being stuck in a traffic jam in the tunnel). In particular, the parametric studies were conducted in the following format: the descent rate was perturbed based on traveling through the tunnel from 50 km/h below the tunnel's posted speed limit to 40 km/h above the limit. Since the descending slopes were specific to each tunnel, the abovementioned values were converted to corresponding specific ranges of descent rates for each tunnel. The initial bubble size was perturbed from 0% to 100% of the globe volume, the aqueous humor production rate from 0.5 to 4 μL/min, the aqueous humor outflow facility from 0 to 2.5 μL/min, and the corneoscleral compliance from 0.5 to 4 μL/mm Hg. In each simulated case, the risk of ocular hypotony with the perturbation of the parameter of the interest was examined while holding all other parameters constant (i.e., using the baseline values for each tunnel). The red dots represent the baseline values for each parameter in Figures 4 to 8.

Results

Changes in the elevation and IOP during travels for all base cases are shown in Figure 2. When the patients arrived at low elevations, the IOP for the simulated travel through the Seikan Tunnel, Bomlafjord Tunnel, and Atlantic Ocean Tunnel dropped to values less than 5 mm Hg, indicating a potential risk for ocular hypotony. Because in our model no negative IOP was allowed,[11] plateau regions with IOP values of 0 mm Hg were predicted in the Bomlafjord Tunnel and Atlantic Ocean Tunnel at low elevations. For simulations where patients travel through the Channel Tunnel and the Ted Williams Tunnel, the minimum IOP was greater than 5 mm Hg. In all simulated base cases, the IOP value increased during the ascent to the tunnel exit and eventually reached the physiologically normal value of 15 mm Hg. A notable exception was the Seikan Tunnel, in which the IOP initially went above 22 mm Hg. Nevertheless, as shown in Figure 3, IOP values for all

Table 3. Constant Values Used in the Theoretical Model Based on Published Data

Symbol	Variable Description	Magnitude	Remarks
$V0_{globe}$	Initial globe volume	7211 mm^3	Calculated using a finite element model[33]
κ	Corneoscleral shell compliance	3.115 μL/mm Hg	Calculated using a finite element model[27,33–35]
μ	Aqueous humor outflow facility	0.25 μL/(min mm Hg)	Experimental values[23–25]
U	Uveoscleral outflow	1.0 μL/min	Experimental values[36]
Q_{Aqu}	Aqueous humor production rate	2.5 μL/min	Experimental values[23,25]
λ	Aqueous humor pseudofacility	0.081 μL/(min mm Hg)	Experimental values[37]

tunnel scenarios reached the normal value of 15 mm Hg within 120 minutes after entering the tunnel.

The influence of the descent rate, ascent rate, bubble size, aqueous humor production rate, outflow facility, and ocular globe compliance on the minimum simulated values of IOP were examined in a series of parametric studies (Figs. 4–8). The results showed that traveling through a short and relatively shallow tunnel similar to the Ted Williams Tunnel is relatively safe, independent of parameter variations. However,

intraocular gas bubbles can increase the risk of ocular hypotony during travel through deeper and longer tunnels, similar to the Bomlafjord Tunnel and Atlantic Ocean Tunnel.

As shown in Figure 4, for the tunnels in which the speed limit was relatively high (i.e., the Seikan Tunnel and Channel Tunnel), the parametric study showed that the descent rate had an inverse relationship with the predicted minimum IOP. On the other hand, in the tunnels with lower speed limits but higher descent
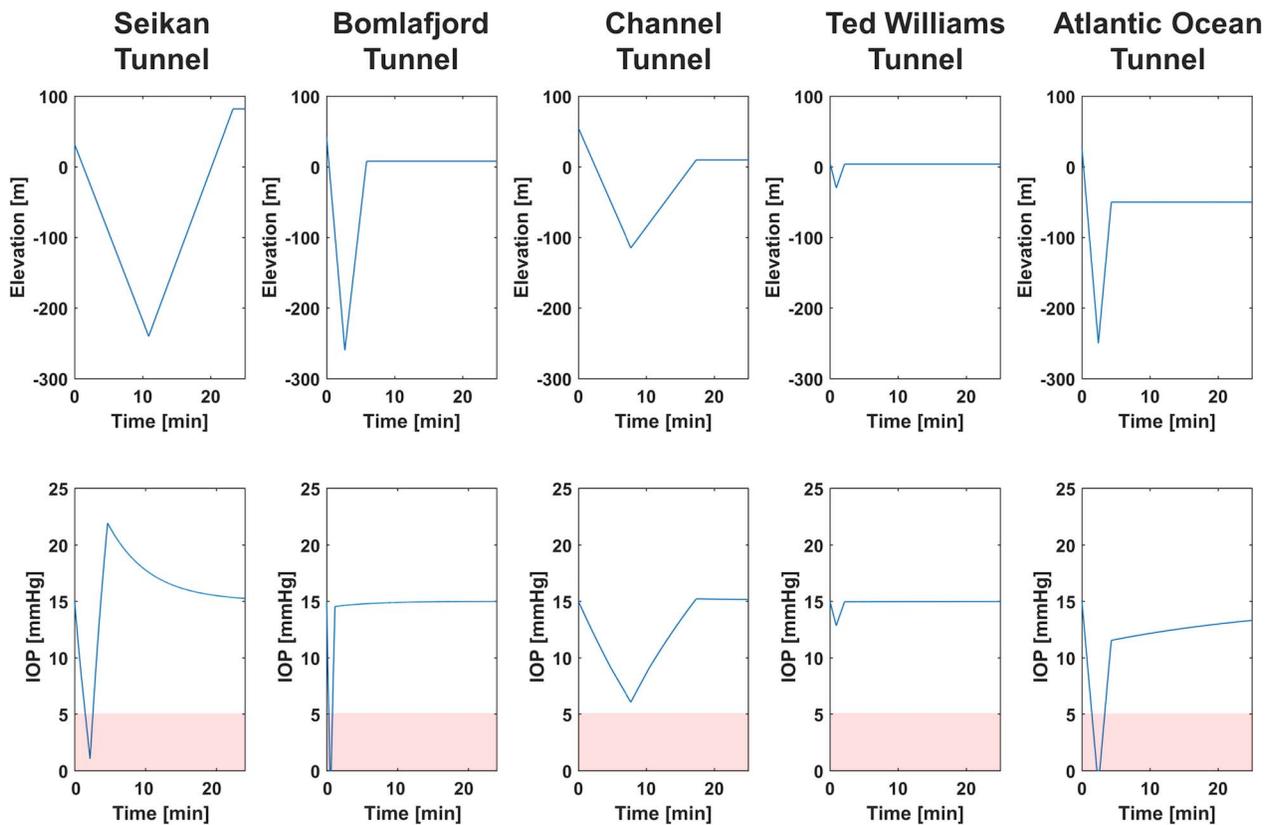

Figure 2. Changes in elevation and IOP versus time for all five simulated tunnels during the first 25 minutes of travel. All subsea tunnels had a profile that showed a descent followed by an ascent. Minimum IOP occurred at the lowest elevations with values of 1.5, 0, 6.9, 12.9, and 0 mm Hg from left to right. The *shaded areas* correspond to the IOP values that put patients at risk for ocular hypotony.
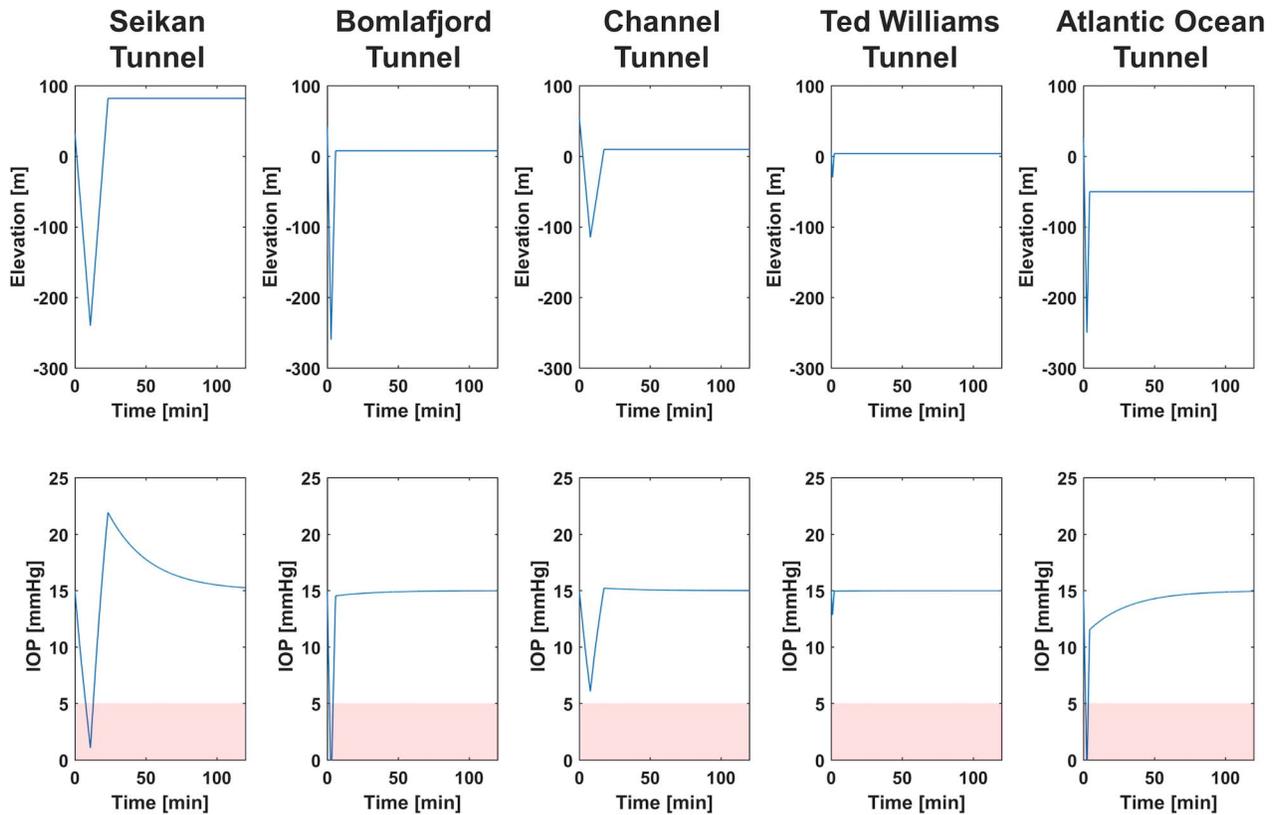
Figure 3. Changes in elevation and IOP during the entire 120 minutes of the travel through the subsea tunnels. The IOP reached slightly higher than 22 mm Hg in the Seikan Tunnel; however, in this tunnel and in all other simulated tunnels, the IOP eventually returned to a physiologically normal value of 15 mm Hg. The *shaded areas* correspond to IOP values that put patients at risk for ocular hypotony.

rates (i.e., Bomlafjord Tunnel and Atlantic Ocean Tunnel), the IOP of travelers with intraocular gas bubbles remained at the minimum theoretical allowable value of 0 mm Hg, indicating that the risk of hypotony was present for all simulated descent rates. The results also showed that a short trip through a relatively shallow tunnel (such as the Ted Williams Tunnel) did not lead to a dangerously low value of the IOP when the descent rate was perturbed.

Because the minimum IOP value always occurred at the lowest part of the tunnel before beginning an ascent, the perturbation of the rate of ascension did not have any influence on the predicted values of the minimum IOP and the potential risk of ocular hypotony (data not shown). However, as shown in our previous work,[9,11] the ascent rate could influence the peak IOP values and the recovery time.

Initial bubble size showed the highest impact on the minimum predicted IOP values among all model inputs as shown in Figure 5. In all tunnels, an increase in bubble size resulted in a drop in the IOP values. With the exception of the Ted Williams Tunnel, in which the patient is never at risk for ocular hypotony,

in all other simulated tunnels, the risk of ocular hypotony can be reduced by reducing the initial bubble size.

To examine how IOP changes with different rates of descent, we simulated a hypothetical case in which the patient travels from a starting elevation of 60 m above sea level (the highest value for the five tunnels we considered) to the lowest elevation of −300 m (the lowest value for the five tunnels we considered). We repeated the simulation for six different descent rates in the range of the rates of travel through the five tunnels in the initial simulations (i.e., 20, 40, 60, 80, 100, and 120 m/min). As shown in Figure 9, in all cases, the IOP dropped to extremely low values, and the descent rate affected the IOP changes only slightly.

As shown in Figures 6 and 7, both increasing the aqueous production rate and increasing the aqueous humor outflow facility had an influence on the predicted values for the minimum IOP as well as the risk of ocular hypotony in most of the simulated cases. While increasing the aqueous humor production rate leads to higher values of minimum IOP, an
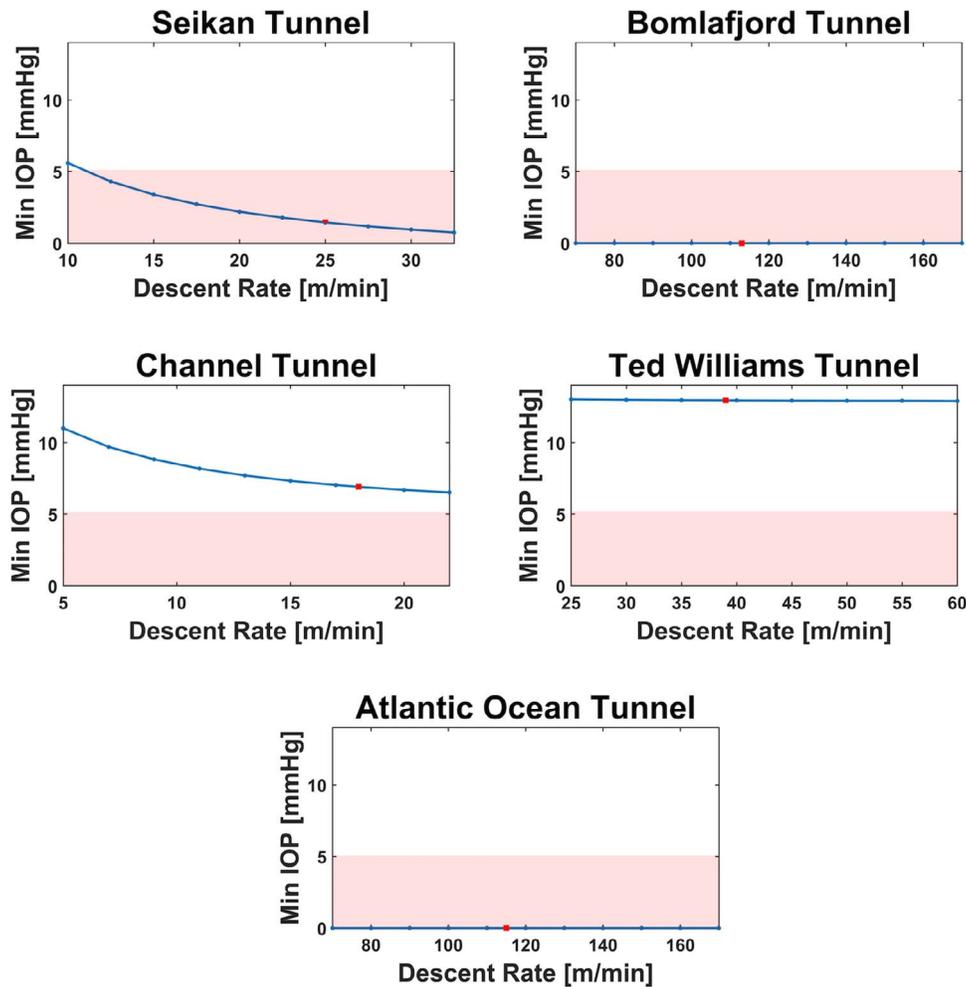
Figure 4. Changes in minimum value of the predicted IOP during travel through the simulated tunnels in response to an alteration of the descent rate. The *shaded areas* correspond to IOP values that put patients at risk for ocular hypotony.

increase in outflow facility further exacerbates the problem and leads to a higher risk of ocular hypotony. For example, in the Channel Tunnel, increasing the aqueous humor production rate or decreasing the outflow facility can bring the IOP slightly above 5 mm Hg, the threshold value for ocular hypotony. However, due to a rapid descent to a relatively low elevation, changes to the two above-mentioned parameters will not eliminate the risk of ocular hypotony in the Seikan Tunnel, Bomlafjord Tunnel, or the Atlantic Ocean Tunnel.

Our parametric study showed that even small values of ocular globe compliance could put patients at risk for hypotony in the Channel Tunnel. Such risks, however, existed for all simulated values of the ocular compliance in the Seikan Tunnel, Bomlafjord Tunnel, and Atlantic Ocean Tunnel (Fig. 8).

Discussion

Previously, it has been shown that exposure to high altitudes could lead to dangerously high values of IOP in patients with intravitreal gas bubbles,[5,7,14] an observation that was confirmed by our theoretical model.[9] In this study, for the first time, we showed that injection of intravitreal gas bubbles may put patients who travel through subsea tunnels at high risk for ocular hypotony. Potential occurrence of transient ocular hypotony during travel through subsea tunnels may negatively affect the vison, which is particularly dangerous if the patient is driving. In addition, ocular hypotony may cause bleeding and/or re-detachment of the repaired retina due to the collapse of the corneoscleral shell. Although this study focuses on travel in subsea tunnels and further research is certainly necessary, we suspect that any
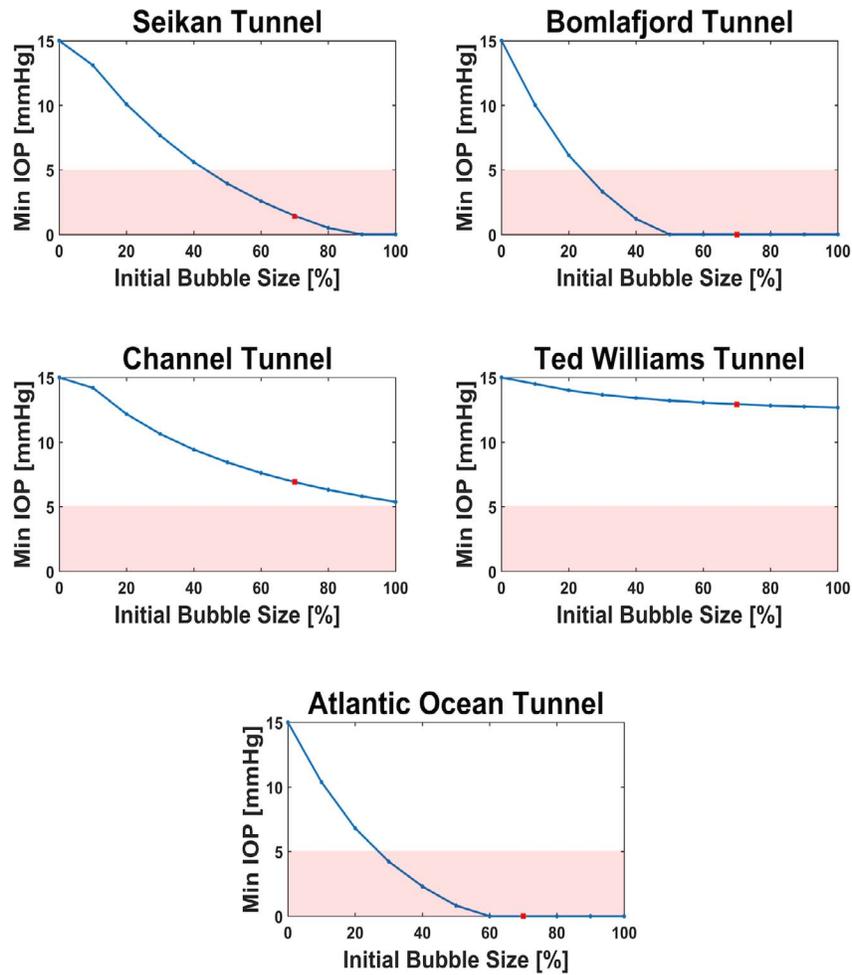
Figure 5. Changes in the minimum value of the predicted IOP during travel through the simulated tunnels in response to alteration of the initial bubble size (%). The *shaded areas* correspond to IOP values that put patients at risk for ocular hypotony.

activity that requires rapid descent to lower elevations (e.g., diving, scuba diving, ski jumping, and bungee jumping) could potentially put patients at risk for ocular hypotony.

Our model predictions of the risk of ocular hypotony greatly depended on the profiles of specific subsea tunnels. Deeper tunnels—such as the Seikan Tunnel, Bomlafjord Tunnel, and the Atlantic Ocean Tunnel, which have low elevation values of −240, −260, and −250 m, respectively—showed more extensive drops in the IOP values, which would increase the risk of hypotony at the lowest elevations. The mechanism of the IOP reduction at the lower elevations can be described as follows: during the descent, the bubble size decreases, subsequently leading to IOP reduction. Although aqueous humor outflow also drops due to its dependency on IOP as a physiological feedback mechanism to maintain normal IOP, the aqueous humor flow changes cannot

entirely compensate for the drop in IOP due to the bubble size reduction. The reason for such a phenomenon is that the changes in the bubble size with elevation are instantaneous, whereas the aqueous humor feedback mechanism has a much slower pace. As shown in our parametric study, a slower descent can help prevent hypotony. Such a case can be observed in the Channel Tunnel: although it is relatively deep (the lowest elevation is −115 m), a slow descent rate of 18 m/min can allow an accumulation of the aqueous humor that is sufficient to maintain the IOP above 5 mm Hg in spite of the instantaneous reductions in bubble size.

It should be noted that the accumulation of the aqueous humor, which is needed to maintain the IOP during the descent, could be problematic. As can be seen in the case of the Seikan Tunnel, increased volume of the aqueous humor along with the bubble size expansion could lead to IOP values above the
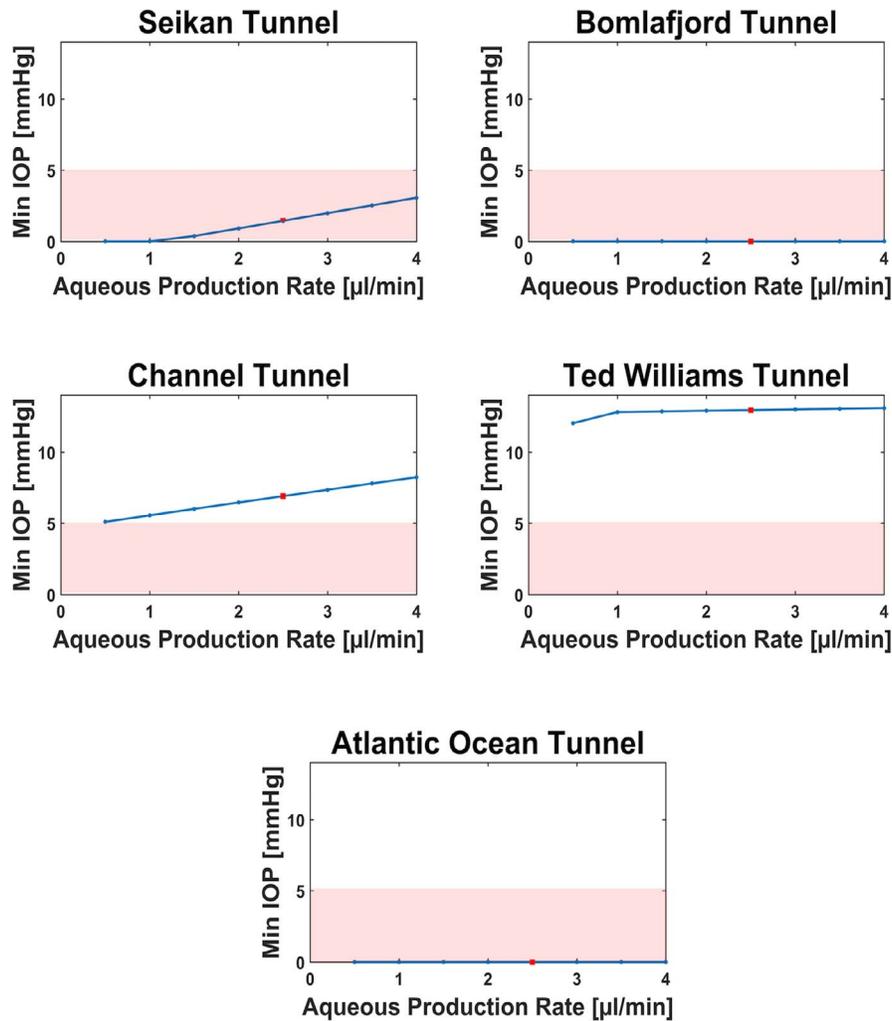
Figure 6. Changes in the minimum value of the predicted IOP during traveling through the simulated tunnels in response to alteration of the aqueous production rate. The *shaded areas* correspond to the IOP values that put the patients at risk for ocular hypotony.

normal value of 15 mm Hg. To avoid high peak IOP values after ascending from the lowest point of the tunnel, the ascent rate should also be kept low so that the eye can compensate for the expansion of the bubble.

Our parametric study also predicted that two of the simulated tunnels, the Bomlafjord Tunnel and the Atlantic Ocean Tunnel, are the most dangerous tunnels to travel in, as compared to other tunnels simulated in this study. In particular, the risk of ocular hypotony can be eliminated only if the intravitreal gas bubble is smaller than 20% of the ocular globe volume. In all other cases for these tunnels, IOP was predicted with values less than 5 mm Hg for all simulated ranges of descent rate, aqueous humor production rate, outflow facility, and ocular compliance (Figs. 4–8).

It should be noted that two of the tunnels (Seikan Tunnel and Channel Tunnel) are rail tunnels that could be used for high-speed trains. The internal pressure of a high-speed train may fluctuate while traveling through a tunnel.[29] In particular, a compression/expansion wave is formed when a train enters/exits the tunnel, and the wave propagates along the tunnel at a nearly sonic speed. This pressure change depends on many factors including the length of the train, the shape of the train, the section of the train in which the patient is seated, the tunnel cross-sectional area, and how well the train car is sealed. This fluctuation in pressure could be as high as 2 kPa and may exceed the pressure changes due to the change in elevation. Such fluctuations are not included in our current model, and our predicted
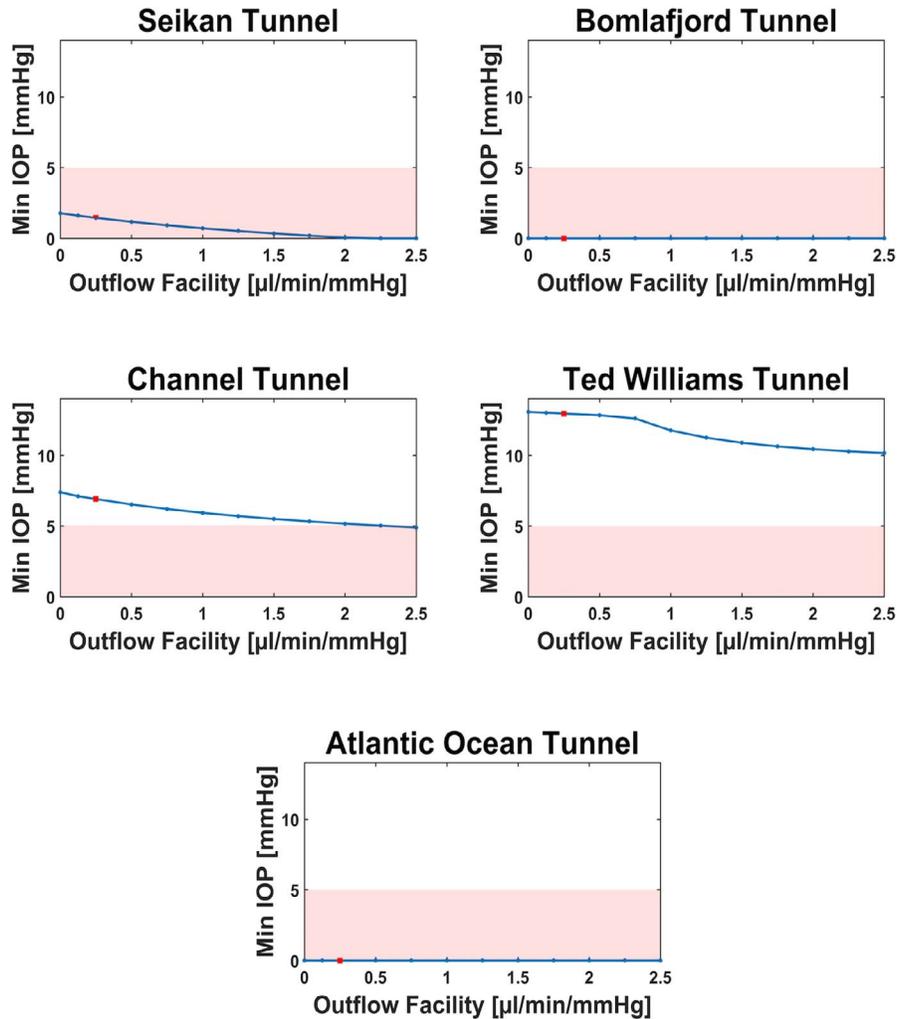
Figure 7. Changes in minimum value of the predicted IOP during travel through the simulated tunnels in response to alteration of the outflow facility. The *shaded areas* correspond to IOP values that put patients at risk for ocular hypotony.

IOP in these tunnels may not reflect the actual IOP of passengers traveling in high-speed trains.[29]

Similar to many other theoretical models, the model used in this study is not free of limitations. We have extensively discussed our model limitations in our previous publications.[9,11] Briefly, our model did not include volume changes due to ocular blood flow. Further, the nonlinearity in the ocular globe in response to IOP changes was not considered; neither were the viscoelastic effects and gas diffusion. Moreover, a fixed outflow facility was used in the model, even though it has been shown that outflow facility is altered with changes in IOP.[30,31] In our previous work,[9,11] we were confident that the above-mentioned limitations did not affect our model predictions significantly because we were able to

closely match the model predictions with clinically and/or experimentally measured values in a number of cases for which those data were available. Although the physical phenomena occurring during the descent portion of the travel through a subsea tunnel is similar in theory to those of our previously validated model, to our best knowledge, no measurements of IOP during travel to lower altitudes are available for case-specific validations. Future experimental measurements of IOP changes during travel to lower elevations will be extremely beneficial for further assessing the accuracy of our theoretical model predictions. Collectively, due the assumptions and simplifications, the exact IOP value predicted by this theoretical model may be different from the clinical measurements of IOP.
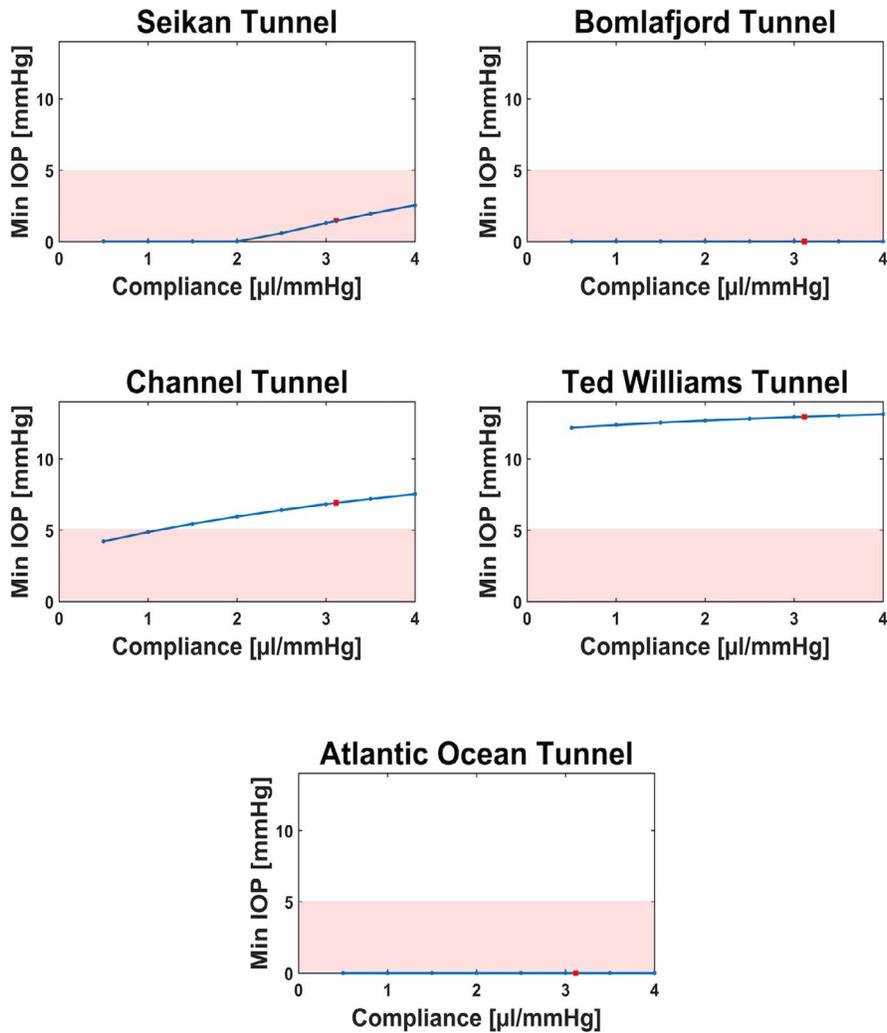
Figure 8. Changes in minimum value of the predicted IOP during travel through the simulated tunnels in response to alteration of the ocular globe compliance. The *shaded areas* correspond to the IOP values that put patients at risk for ocular hypotony.
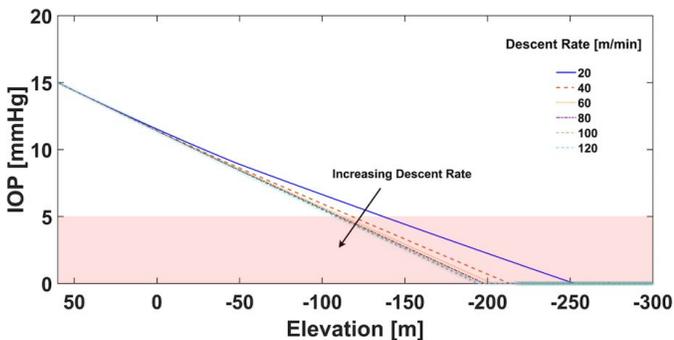

Figure 9. IOP changes versus elevation for a number of different descent rates within the range of those used in the five simulated tunnels.

In summary, our simulation showed that traveling through subsea tunnels can put patients with intravitreal gas bubbles at risk for ocular hypotony. Such risk mainly depends on the change in elevation during travel, the descent rate, and the initial bubble size. Smaller changes in elevation, slower descent rates, and smaller sizes for the injected bubbles can be considered to avoid extreme IOP reductions. Although future experimental measurements could increase the level of confidence in our theoretical model, we believe that cautioning patients to avoid travel through deep subsea tunnels may be necessary to avoid ocular hypotony following the injection of intravitreal gases.

Appendix

The governing equations of the system were developed as described below:

The change in bubble volume ΔV_B was defined as the sum of change in the ocular globe volume ΔV_{globe} and the change in the aqueous humor volume ΔV_{Aqu}:

$$\Delta V_B = \Delta V_{globe} + \Delta V_{Aqu} \qquad (1)$$

The change in bubble volume was also defined as

$$\Delta V_B = V_B - V0_B, \qquad (2)$$

where V_B is the bubble volume and $V0_B$ is the initial bubble volume.

Using Boyle's law and assuming isothermal pressure/volume changes, we defined the volume of the gas bubbles V_B as the following:

$$V_B = V0_B \frac{P0_{in}}{P_{in}}. \qquad (3)$$

The initial bubble volume $V0_B$ was reported as a percentage of initial globe volume $V0_{globe}$:

$$V0_B = \alpha_0 V0_{globe}. \qquad (4)$$

Equations (2), (3), and (4) were then combined:

$$\Delta V_B = \alpha_0 V0_{globe} \frac{P0_{in}}{P_{in}} - \alpha_0 V0_{globe}. \qquad (5)$$

The change in the globe volume $V0_{globe}$ was also calculated based on a compliance factor κ (obtained from a finite element–based pressure volume curve of the globe, as described previously[9,11,33]) and the change in the gauge intraocular pressure (*Gauge IOP*):

$$\Delta V_{globe} = \kappa(\Delta Gauge\ IOP). \qquad (6)$$

The pressure difference between the absolute intraocular pressure P_{in} and the absolute exterior air pressure P_{out} was defined as *Gauge IOP*, and the change in *Gauge IOP* from the initial elevation (i.e., $\Delta Gauge\ IOP$) was written as:

$$\Delta Gauge\ IOP = (P_{in} - P_{out}) - (P0_{in} - P0_{out}). \qquad (7)$$

Equations (6) and (7) were then combined:

$$\Delta V_{globe} = \kappa(P_{in} - P_{out} - P0_{in} + P0_{out}). \qquad (8)$$

ΔV_B and ΔV_{globe} from Equations (5) and (8) were then substituted into Equation (2):

$$V0_B \frac{P0_{in}}{P_{in}} - V0_B - \kappa(P_{in} - P0_{in} - P_{out} + P0_{out})$$
$$- \Delta V_{Aqu}$$
$$= 0. \qquad (9)$$

By multiplying Equation (9) by P_{in}, we obtained a quadratic governing equation:

$$V0_B P0_{in} - V0_B P_{in} - \kappa P_{in}(P_{in} - P0_{in} - P_{out} + P0_{out})$$
$$- \Delta V_{Aqu} P_{in}$$
$$= 0, \qquad (10)$$

Or, when arranged by the unknown pressure P_{in} and after using Equation (4):

$$\kappa P_{in}^2$$
$$- \left(\kappa P0_{in} + \kappa P_{out} - \kappa P0_{out} - \alpha_0 V0_{globe} - \Delta V_{Aqu}\right) P_{in}$$
$$- \alpha_0 V0_{globe} P0_{in}$$
$$= 0. \qquad (11)$$

The rate of the other unknown in Equation (11), which is the change in the aqueous humor total volume in the ocular globe ΔV_{Aqu}, was calculated based on the inflow rate and outflow rate of the aqueous humor (note that $\frac{dV_{Aqu}}{dt} = \frac{d}{dt}(\Delta V_{Aqu})$ since $V_{Aqu} = V0_{Aqu} + \Delta V_{Aqu}$ and $V0_{Aqu}$, i.e., the initial aqueous humor volume, is not a function of time):

$$\frac{d}{dt}(\Delta V_{Aqu}) = outflow\ rate - inflow\ rate, \qquad (12)$$

Where the inflow rate was given by the aqueous production rate Q_{Aqu} minus a pressure dependent term for pseudofacility λ:

$$inflow\ rate = Q_{Aqu} - \lambda(P_{in} - P_{out} - P0_{in} + P0_{out}). \qquad (13)$$

The outflow facility μ, absolute episcleral venous pressure P_e, and a pressure independent term for uveoscleral outflow U were used to define the outflow rate:

$$outflow\ rate = \mu(P_{in} - P_e) + U. \qquad (14)$$

The second governing equation of the system was obtained by combining Equations (12), (13), and (14):

$$\frac{d}{dt}\left(\Delta V_{Aqu}\right) = \mu(P_{in} - P_e) + U$$
$$- \left[Q_{Aqu} - \lambda(P_{in} - P_{out} - P0_{in} + P0_{out})\right]. \qquad (15)$$

The above differential equation [Equation (15)] along with the quadratic equation [Equation (11)] were solved simultaneously for the unknown values of P_{in} and ΔV_{Aqu}. The quadratic formula and Euler's method were used to solve these equations using internally developed codes in MATLAB (Math-Works, Natick, MA). Since P_{in} is an absolute pressure value, only the positive root of the quadratic equation was acceptable. Other parameters that are used in the above equations are described in Table 2, and the numerical values used for the constants are listed in Table 3. In addition, the barometric formula[37] was used to calculate the absolute exterior air pressure P_{out}:

$$P_{out} = 0.1013\ (1-2.26 \times 10^{-5}h)^{5.26}\ \text{MPa}$$
$$= 759.8\ (1-2.26 \times 10^{-5}h)^{5.26}\ \text{mm Hg} \qquad (16)$$

where h is the elevation. The initial elevation was used to calculate the initial exterior pressure. In addition, a constant gauge episcleral venous pressure of 9 mm Hg at all elevations was used to calculate the absolute episcleral venous pressure P_e:

$$P_e = P_{out} + 9\ \text{mm Hg} \qquad (17)$$

Finally, a 15-mm Hg pressure difference between the absolute interior and exterior pressures was used to calculate the initial absolute intraocular pressure $P0_{in}$:

$$P0_{in} = P0_{out} + 15\ \text{mm Hg}. \qquad (18)$$

References

1. Hatef E, Sena DF, Fallano KA, Crews J, Do DV. Pneumatic retinopexy versus scleral buckle for repairing simple rhegmatogenous retinal detachments. *Cochrane Database Syst Rev*. 2015;5:8350.

2. Mitry D, Charteris DG, Fleck BW, Campbell H, Singh J. The epidemiology of rhegmatogenous retinal detachment: geographical variation and clinical associations. *Br J Ophthalmol*. 2010;94:678–684.

3. Chan CK, Lin SG, Nuthi AS, Salib DM. Pneumatic retinopexy for the repair of retinal detachments: a comprehensive review (1986–2007). *Surv Ophthalmol*. 2008;53:443–478.

4. Nemet A, Moshiri A, Yiu G, Loewenstein A, Moisseiev E. A review of innovations in rhegmatogenous retinal detachment surgical techniques. *J Ophthalmol*. 2017;2017:4310643.

5. Lincoff H, Weinberger D, Reppucci V, Lincoff A. Air travel with intraocular gas: I. The mechanisms for compensation. *Arch Ophthalmol*. 1989;107:902–906.

6. Forrester JV, Dick AD, McMenamin PG, Roberts F, Pearlman E. *The Eye: Basic Sciences in Practice*. New York: Elsevier; 2016.

7. Kokame GT, Ing MR. Intraocular gas and low-altitude air flight. *Retina*. 1994;14:356–358.

8. Fang I-M, Huang J-S. Central retinal artery occlusion caused by expansion of intraocular gas at high altitude. *Am J Ophthalmol*. 2002;134:603–605.

9. Amini R, Barocas VH, Kavehpour HP, Hubschman JP. Computational simulation of altitude change-induced intraocular pressure alteration in patients with intravitreal gas bubbles. *Retina*. 2011;31:1656–1663.

10. Sommer A. Glaucoma risk factors observed in the Baltimore Eye Survey. *Curr Opin Ophthalmol*. 1996;7:93–98.

11. Gsellman L, Amini R. Patients with intravitreal gas bubbles at risk of high intraocular pressure without exceeding elevation of surgery: theoretical analysis vitrectomy, high IOP, and no high altitude travel. *Invest Ophthalmol Vis Sci*. 2016;57:3340–3347.

12. Brosh K, Strassman I, Seelenfreund M. High intraocular pressure in four vitrectomized eyes with intravitreal C3F8 without high altitude travel. *Eye*. 2014;28:892.

13. Tseng VL, Kim CH, Romero PT, et al. Risk factors and long-term outcomes in patients with low intraocular pressure after trabeculectomy. *Ophthalmology*. 2017;124:1457–1465.

14. Lincoff H, Weinberger D, Stergiu P. Air travel with intraocular gas: II. Clinical considerations. *Arch Ophthalmol*. 1989;107:907–910.

15. Mills MD, Devenyi RG, Lam W-C, Berger AR, Beijer CD, Lam SR. An assessment of intraocular pressure rise in patients with gas-filled eyes during

simulated air flight. *Ophthalmology*. 2001;108:40–44.

16. Kokame GT, Ing MR. Intraocular gas and low-altitude air flight. *Retina (Philadelphia, Pa)*. 1994;14:356–358.

17. Ribeiro e Sousa L. Learning with accidents and damage associated to underground works. In: Campos e Matos A, Ribeiro e Sousa L, Kleberger J, Lopes Pinto P, eds. *Geotechnical Risk in Rock Tunnels: Selected Papers From a Course on Geotechnical Risk in Rock Tunnels, Aveiro, Portugal, 16–17 April 2004*. New York: Taylor & Francis, 2003;7.

18. Martinsen S. Success story at Bomlafjord. *Tunnels Tunnelling Int*. 2000;32.

19. Indrehus O, Aralt TT. Air quality and ventilation fan control based on aerosol measurement in the bi-directional undersea Bmlafjord Tunnel. *J Environ Monitoring*. 2005;7:349–356.

20. Eisenstein Z. Large undersea tunnels and the progress of tunnelling technology. *Tunnelling Underground Space Technol*. 1994;9:283–292.

21. Vaghar S, Bobrow DJ. Comparison of two excavation support systems in clay: Central Artery Tunnel, Boston, Massachusetts, USA. Paper No. 6.09. *Proceedings of the Fourth International Conference on Case Histories in Geotechnical Engineering*. St. Louis, MO, March 9–12, 1998.

22. Lancellotti AR, Grantz WC. From concept to completion: The Ted Williams Tunnel. Immersed Tunnel Techniques 2. *Proceedings of the International Conference Organized by the Institution of Civil Engineers in Association with the Institution of Engineers of Ireland*. Cork, Ireland, April 23–24, 1997.

23. Sit AJ, Nau CB, McLaren JW, Johnson DH, Hodge D. Circadian variation of aqueous dynamics in young healthy adults. *Invest Ophthalmol Vis Sci*. 2008;49:1473–1479.

24. Toris CB, Yablonski ME, Wang Y-L, Camras CB. Aqueous humor dynamics in the aging human eye. *Am J Ophthalmol*. 1999;127:407–412.

25. Epstein D, Allingham R, Schuman J. Segmental nature of outflow: implication for angle closure glaucoma. In: Epstein DL, Allingham RR, Schuman JS, eds. *Chandler and Grant's Glaucoma, 4th ed*. Baltimore, MD: Williams & Wilkins; 1997:20–21.

26. Johnstone MA, Grant WM. Pressure-dependent changes in structures of the aqueous outflow system of human and monkey eyes. *Am J Ophthalmol*. 1973;75:365–383.

27. Silver DM, Geyer O. Pressure-volume relation for the living human eye. *Curr Eye Res*. 2000;20:115–120.

28. Sigal IA, Flanagan JG, Ethier CR. Factors influencing optic nerve head biomechanics. *Invest Ophthalmol Vis Sci*. 2005;46:4189–4199.

29. Martínez A, Vega E, Gaite J, Meseguer J. Pressure measurements on real high-speed trains travelling through tunnels. In: *Proceedings of BBAA VI International Colloquium on Bluff Bodies Aerodynamics & Applications*. Milano, Italy, 2008.

30. Armaly MF. The effect of intraocular pressure on outflow facility. *Arch Ophthalmol*. 1960;64:125–132.

31. Lei Y, Overby DR, Boussommier-Calleja A, Stamer WD, Ethier CR. Outflow physiology of the mouse eye: pressure dependence and washout. *Invest Ophthalmol Vis Sci*. 2011;52:1865–1871.

32. Ohio Supercomputer Center. 1987. Ohio Supercomputer Center. Columbus, OH: Ohio Supercomputer Center. http://osc.edu/ark:/19495/f5s1ph73.

33. Amini R, Barocas VH. Anterior chamber angle opening during corneoscleral indentation: the mechanism of whole eye globe deformation and the importance of the limbus. *Invest Ophthalmol Vis Sci*. 2009;50:5288–5294.

34. Pierscionek BK, Asejczyk-Widlicka M, Schachar RA. The effect of changing intraocular pressure on the corneal and scleral curvatures in the fresh porcine eye. *Br J Ophthalmol*. 2007;91:801–803.

35. Liu J, He X. Corneal stiffness affects IOP elevation during rapid volume change in the eye. *Invest Ophthalmol Vis Sci*. 2009;50:2224–2229.

36. Alm A, Nilsson SF. Uveoscleral outflow–a review. *Exp Eye Res*. 2009;88:760–768.

37. Kaufman PL. Enhancing trabecular outflow by disrupting the actin cytoskeleton, increasing uveoscleral outflow with prostaglandins, and understanding the pathophysiology of presbyopia: Interrogating Mother Nature: asking why, asking how, recognizing the signs, following the trail. *Exp Eye Res*. 2008;86:3–17.

38. Atmosphere USS. Washington, DC: US Government Printing Office. Available in hard copy from the National Technical Information Office, Springfield, Virginia (Product Number: ADA-035-6000); 1976.